Available online at www.sciencedirect.com
SCIENCE DIRECT®

Journal of the European Ceramic Society 24 (2004) 3327–3335
www.elsevier.com/locate/jeurceramsoc

Materials based on nanosized β-Si_3N_4 composite powders

M. Herrmann[a,*], I. Schulz[b], I. Zalite[c]

[a]*Fraunhofer-Institut für Keramische Technologien und Sinterwerkstoffe, Winterbergstr 28, D-01277 Dresden, Germany*
[b]*Technical University, Dresden, Germany*
[c]*Institute of Inorganic Chemistry, Riga Technical University, Salaspils, Latvia*

Abstract

Nanomaterials offer the possibility to improve properties like hardness, wear resistance or offer some advantages in production and microstructure formation. The commercial realisation of such materials depends on the one hand on the realisation of improved properties, on the other hand on realisation of the production of powders having constant properties with acceptable prices, as well as reproducible processing. The use of nonoxide nanopowders request additionally a careful control of the oxygen content. In this paper the concept of production of nano β-Si_3N_4 composite powders containing besides the nano crystallites of β-Si_3N_4, also the grain boundary phase, their processing and resulting microstructures are discussed. The grain boundary phase coating the surface of the powders protect them from further hydrolysis. This possibility allows the production of nanostructured Si_3N_4-ceramics or composites. The densification of such powders, microstructures and properties will be explained.

Keywords: Coated powders; Nanocomposites; Powders; Si_3N_4; Sintering

1. Introduction

Silicon nitride ceramics have been intensively studied for many years because of their great potential for structural applications at room and high temperatures. This is due to their excellent mechanical properties in combination with good corrosion and thermal shock resistance. Over the past decade a continuous increase in the number of application fields has been observed.[1,2] Recently an increased wear resistance of nano silicon nitride was observed.[3,4]

At present the possibilities which nanopowders and nanomatetrials offer are widely discussed. Such possibilities include the reduction of sintering temperatures, improved properties such as hardness, wear resistance, new possibility of designing new structures or composite materials.[5] The disadvantages of the nanopowders, namely the difficulties of processing of such powders with conventional technologies, the high price of the powders and the problems with the oxygen pick up of nonoxide nanopowders during the processing, strongly retard the development and application of such materials.

The production of nanosized Si_3N_4 materials can be realised by special sintering techniques like spark plasma sintering[6] or by using amorphous powders in combination with the retarding of the grain growth due to pinning by SiC.[7] If standard sintering techniques are used, the starting Si_3N_4-powder must be a β-Si_3N_4 powder because the phase transformation during the liquid phase sintering results in grain growth.[8,9] The plasmachemical synthesis of Si_3N_4 powders[10] makes it possible to economically produce nanosized Si_3N_4 powders. However, the relationship between powder, processing, microstructure and properties of the resulting materials are still under investigation.

The aim of this work is to show some possibilities to overcome the processing problems of Si_3N_4-nanopowders and to investigate the structure formation in nanosized Si_3N_4 materials.

2. Experimental

The nanosized nitride powders and their composites are prepared by evaporation of commercially available Si powder (with a mean grain size of 10–20 μm), and the sintering additive into a radio-frequency inductively-coupled nitrogen plasma and subsequent condensation of the products during quenching. This process is a

* Corresponding author.
E-mail address: mathias.herrmann@ikts.fhg.de (M. Herrmann).

0955-2219/$ - see front matter © 2003 Elsevier Ltd. All rights reserved.
doi:10.1016/j.jeurceramsoc.2003.10.049

special type of a direct nitridation of Si at high temperatures. The resulting powder is mostly amorphous and has surface area of 30–100 m^2/g depending on the reaction conditions. The process is described in detail in Ref 10.

The used β-powders were synthesised from Si in the presence of 6 wt.% Y_2O_3 and 3.2 wt.% Al_2O_3. The powder PP1 contains amorphous silicon nitride, besides α- and β-Si_3N_4. The as-synthesised plasmachemical powders contain a high amount of amorphous silicon nitride (75–80 wt.%) The crystallised powders PP2 and PP3 contains only crystalline Si_3N_4, mostly β-Si_3N_4 (Table 1, Fig. 1). For the samples with changed additive content additionally Y_2O_3 (grade fine; HC Stark) and Al_2O_3 (AKP 50; Sumitomo) were added. The mixing was carried out in a planetary ball mill in isopropanol. Additionally, commercial α-Si_3N_4 powders (Baysinid, Bayer AG; SNE-10, UBE) were used for comparison (Table 1).

For gas-pressure sintering, the samples were cold-isostatically pressed into bars ($20\times20\times60$ mm^3) at a pressure of 200 MPa. In a first set of materials the additive content was varied and the sintering behaviour was determined (Table 2). A second set of materials with a higher additive content (9 mass% Y_2O_3 and 5 mass% Al_2O_3) was sintered at 1750 °C for 90 min. Under these conditions, the materials have a density higher than 99% theoretical density and the conversion of α to β-Si_3N_4 is complete. The samples were then heat treated at 1750, 1825 and 1900 °C at different times (Table 3).

Table 1
Characteristics of the used powders

Powder	Production method		Surface area (BET) (m^2/g)	β/(α + β) (%)	Crystallite size (nm)	Amorphous (%)
PP1	PCH	As synthes.	70	6	20±3	80
PP2	PCH	Crystallised	11	70	53±5	
PP3	PCH	Crystallised	10	69	61±5	
BAYSINID	GP		12	4.2	50±5	
SNE 10	Diimide		10.7	1.5	45±5	

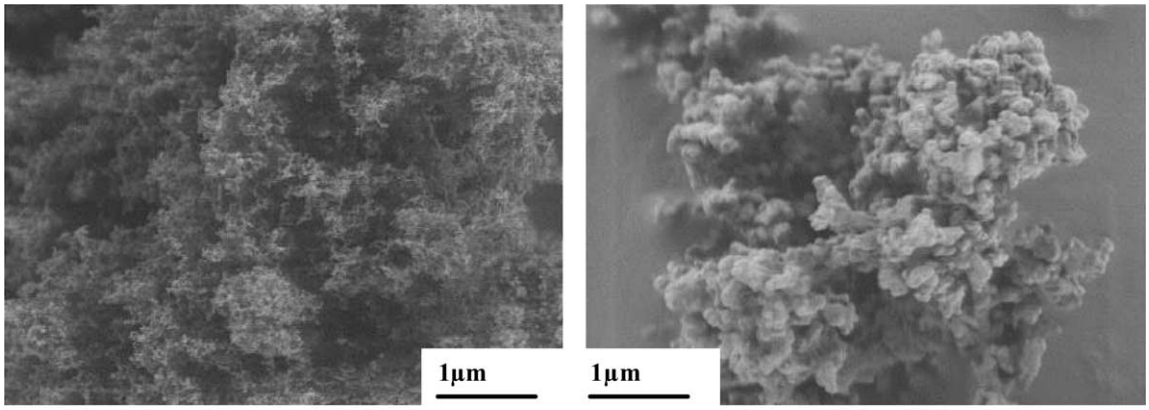

Fig. 1. SEM micrograph of a powder (a) as-synthesised and (b) crystallised at 1500 °C.

Table 2
Densities and Properties of materials sintered at different temperatures

T (°C)	E10 + 6 Y/3.2 Al	PP3 + 6 Y/3.2 Al			PP3 + 5.6 Y/5.5Al		
	ρ/ρ_{th} (%)	ρ/ρ_{th} (%)	σ_{4b} (MPa)	K_{IC} ($MPam^{1/2}$)	ρ/ρ_{th} (%)	σ_{4b} (MPa)	K_{IC} ($MPam^{1/2}$)
1600	92.7	95.5	470	3.6	99.0	660	3.5
1650	95.2	99.9	715	4.0	99.9	765	3.8
1700	97.0	99.9	–	4.2	99.9	800	4.3

Table 3
Microstructures and properties of materials made from the Baysinid and PP2 powders sintered at different temperatures

Powder	Sintering conditions		H_{V10}	K_{IC} (MPa $m^{1/2}$)	d_{50} (μm)	d_{90} (μm)	A > 6.5[a]
	T (°C)	Time (min)					
Baysinid	1750	90	1466	5.1	0.31	0.68	9
PP2			1478	5.3	0.17	0.36	11
Baysinid	1825	180	1399	5.6	0.52	1.05	24
PP2			1411	6.3	0.49	1.04	23
Baysinid	1900	10	1421	5.3	0.32	0.68	11
PP2			1436	5.9	0.26	0.46	13
Baysinid	1900	90	1344	5.9	0.53	1.15	31
PP2			1368	5.9	0.48	1.05	22

[a] Percentage of grains with an aspect ratio (A) > 6.5.

Table 4
Microstructures and properties of materials from different powders hot pressed at 1700 °C

Powder	β/(α + β) (%)	Grain thickness (μm)		Grains with A > 5.5[a]	Strength, σ_{4b} (MPa)	K_{IC} (MPa$m^{1/2}$)	H_{V10}
		d_{50}	d_{90}				
PP2	100	0.08	0.15	10	671 ± 83	3.2	1620
50% SNE-10/50% PP2	90	0.07	0.17	32	756 ± 65	3.5	1670
SNE-10	71	0.12	0.28	19	968 ± 15	4.5	1690

[a] Percentage of grains with an aspect ratio (A) higher than 5.5.

A third set of materials was hot pressed at 1700 °C. The materials were produced from the plasmachemically synthesised powders PP2 and mixtures of these powders with the powder SN-E10 (Table 4). XRD measurement (CuK_α-radiation, Ni filter) and Rietveld refinement (Autoquan ++) was used to determine the crystallite size and the phase content of the powders. The HV10 Vickers hardness was determined. The fracture toughness was calculated according to the equation derived by Anstis.[11] Other details regarding the preparation and analysis of the materials are provided elsewhere.[4]

3. Results

3.1. Sintering and microstructure formation

The plasmacheminal synthesised powders with different additive content were sintered in a gas pressure furnace at different temperatures in the range of 1600 up to 1900 °C.

The Fig. 2 shows the densification kinetics of the materials during the gas pressure sintering. The sintering of the sample made of plasmachemical powders started earlier than the sample made of the E10 powder. The maximum shrinkage rate was lower than that of for the E10 powder. Nevertheless, the materials made from the nanosized powders reached a density of more than 99% of the theoretical density faster than the materials based on E10 powder (Table 2). With a higher additive content the densification can be achieved at temperatures even as low as 1600 °C. In the samples no signs of preferential sintering inside the composite powder particles is visible (Fig. 3).

The set of materials with a higher additive content (9 mass % Y_2O_3 and 5 mass % Al_2O_3) was sintered and heat treated at 1750, 1825 and 1900 °C for different times. The resulting properties and microstructures are shown in Fig. 4 and in Table 3.

For the materials based on the β-powder at 1600–1700 °C nanosized grains with a low aspect ratio were observed. At 1750–1825 °C sintering temperatures a

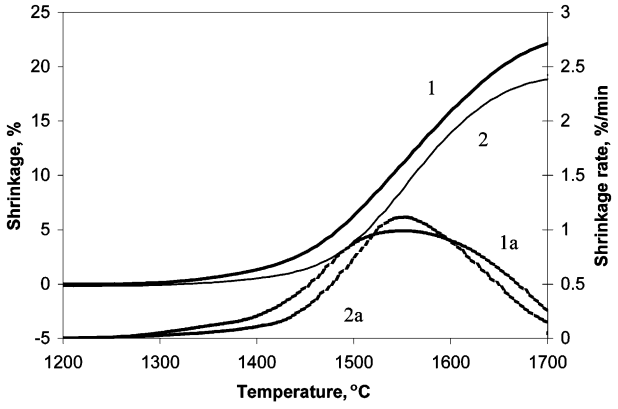

Fig. 2. Shrinkage (1,2) and shrinkage rate (1a,2a) of materials made of PP3 (1,1a) and E 10 powder (2,2a) (heating rate: 10 K/min; additive content 5.6Y_2O_3 5.5% Al_2O_3).

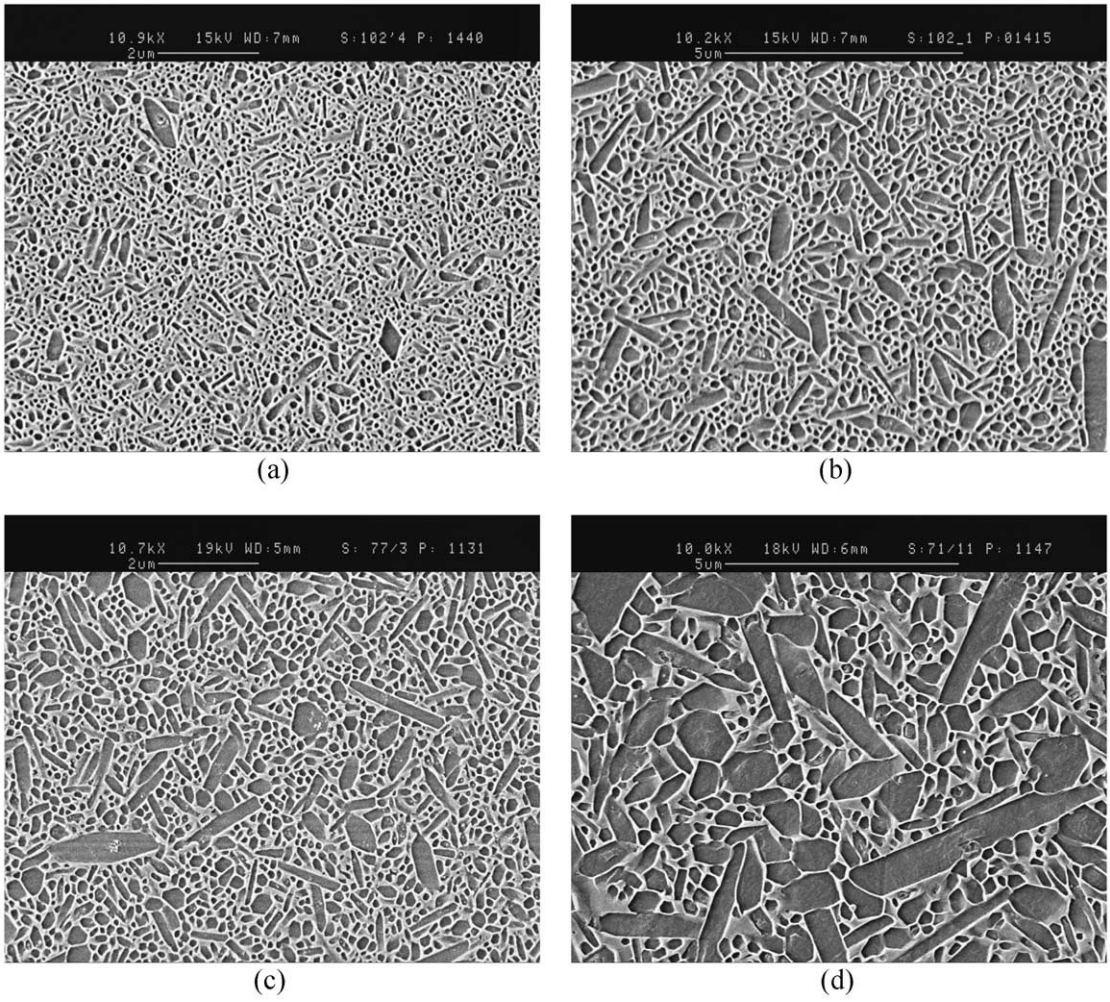

Fig. 3. SEM micrographs of etched, polished cross sections of sintered PP2 + 5.6Y_2O_3 5.5% Al_2O_3 sintered at 1600 °C (a) and sintered at 1700 °C PP2 + 5.6Y_2O_3 5.5% Al_2O_3 (b) PP2 + 6% Y_2O_3 3.2% Al_2O_3 (c) and E10 + 9Y_2O_3 5% Al_2O_3 (d).

lower grain size, a higher amount of elongated grains and a higher fracture toughness could be realised in the materials based on the nano β-powders (Tables 2 and 3). After sintering at higher sintering temperatures or longer sintering times, the structures and properties are similar, regardless of the α/β ratio in the starting powder (Fig. 4c and d).

A set of materials, hot pressed at 1700 °C, was produced from the plasmachemically synthesised powders PP2 and mixtures of these powders with the powder SN-E10. The resulting microstructures and properties are given in Table 4 and Fig. 5. The results demonstrate that the materials produced from the β-powder had finer grain sizes and narrower grain size distributions than the other powders. The grain size distributions of the materials produced by pure plasmachemically synthesised powders were very similar to those of the PP2/50 mass % SN-E10 powder mixtures (Table 4 and Fig. 5), showing the decisive role of the amount of β-seeds.

4. Discussion

The crystallisation of the amorphous Si_3N_4 powder without additives resulted in mainly α-Si_3N_4 at 1300–1500 °C. At higher temperatures β-Si_3N_4 was formed in the sub-μm region.[10] The production of nanosized β-powders was possible by the crystallisation in the presence of sintering additives. Under crystallisation conditions these additives form a oxynitride liquid and change the crystallisation path to nanosized β-Si_3N_4. The oxynitride liquid formed at these temperatures accelerate the crystallisation but is viscous enough to prevent intensive grain growth. An indication for this is that, after the crystallisation no change of the α/β ratio during further heat treatment was observed.[8] In the crystallised powder the nanosized β-crystallites are embedded in a oxynitride amorphous phase. The formation of such composite powders has two advantages on the one side the formed composite particles are in the μm range and can be processed like conventional

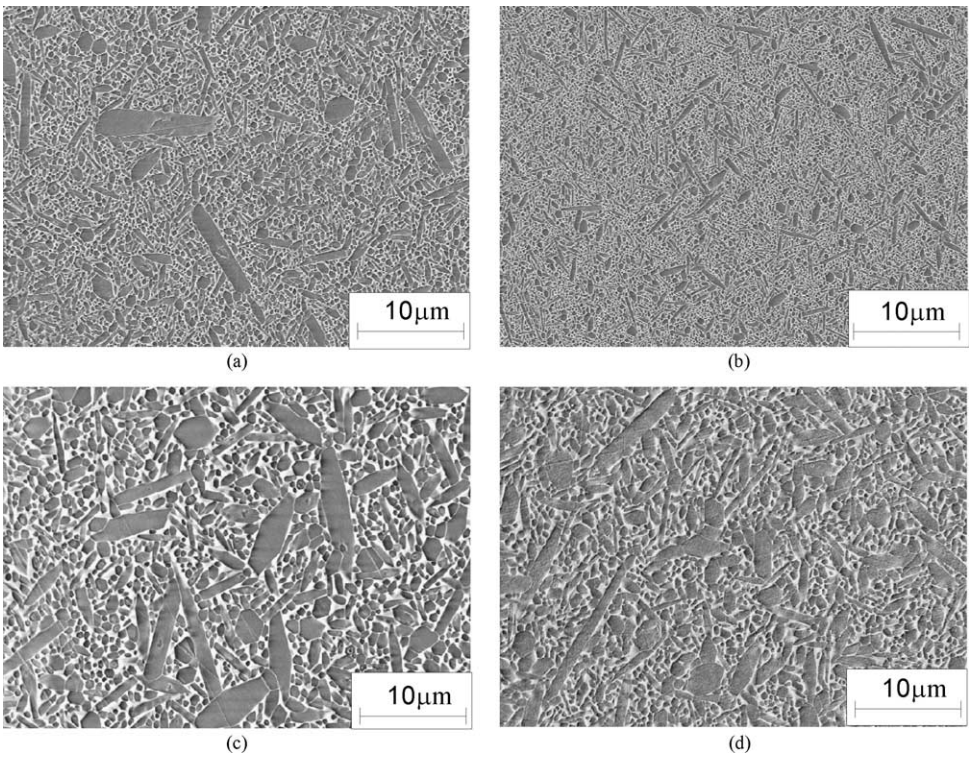

Fig. 4. SEM micrographs of etched, polished cross sections of sintered materials produced from the Baysinid powder (a, c) and by the plasma-chemically synthesised powder PP3 (b, d) at different sintering conditions 1750 °C 90 min (a, b), 1900 °C 90 min (c, d).

powders, on the other side the covering by the oxynitride liquid results in better stability against hydrolysis and oxygen pick up. In the samples no signs of preferential sintering and grain growth inside the grains is visible, as is common for the solid phase sintering of agglomerated powders. The reason is the primary and secondary rearrangement of the powders during early stage of sintering, when the viscosity of the liquid is high enough to prevent the grain growth. The microstructures of the materials produced under different sintering conditions show that the microstructure of the materials produced from nano-β powder can be varied in a wide range, from very fine microstructures to in-situ-reinforced microstructures (Fig. 4, Table 3).

Large differences exist between the materials produced from α-and β-Si_3N_4 powders sintered at low sintering temperatures. The main reason for this behaviour are the different densities of β-nuclei. In the materials made from high α-Si_3N_4 during early steps of sintering the metastable α-Si_3N_4 dissolves and precipitates on existing β-Si_3N_4 nuclei. Due to the low amount of growing nuclei a relativly fast anisotropic grain growth is observed during the phase transformation under normal sintering conditions.[1,9,12]

Only during spark plasma sintering at low temperatures a transformation with a low growth rate was observed.[5] In the case of high density of β-nuclei, the microstructure becomes finer. However, the resulting grain size cannot be directly related to the starting density of nuclei. In the α-powder, predominantly α-Si_3N_4 dissolves in the liquid to saturate it with silicon nitride. On the contrary, in the β-powder, a higher amount of β-Si_3N_4 dissolves in the liquid to reach the saturation. The influence of the density of β-nuclei and the amount of α-Si_3N_4 on the microstructure can be derived from the analysis of the hot pressed mixtures of the plasma-chemically produced powder and the E10 powder (Fig. 5, Table 4). The addition of only 50% of the plasmachemically produced powder to the starting α-Si_3N_4 powder results in a very fine microstructure of the hot pressed materials due to the high density of growing β-nuclei. On the other side, the microstructure of the material made from the pure plasmachemical powder PP2 results in nearly the same grain size distribution but lower aspect ratio. In the mixed powder, initially (at the beginning) the density of β-nuclei is lower than in the PP2 powder, but these nuclei are stabilised during the heating by the higher amount of dissolving α-Si_3N_4. The growth rate in the thickness was observed to be 6–30 times lower than the growth rate in length.[13–16] Therefore it was found that the β-nuclei grow during the α/β transformations e.g. under high supersaturation mainly in the longitudinal direction, resulting in a rapid increase in the aspect ratio.

The heat treatment of the materials with 9 mass % Y_2O_3 and 5 mass % Al_2O_3 at 1750 °C, 1825 °C and 1900 °C showed that after the α-β conversion an anisotropic grain growth takes place. The growth rates in the

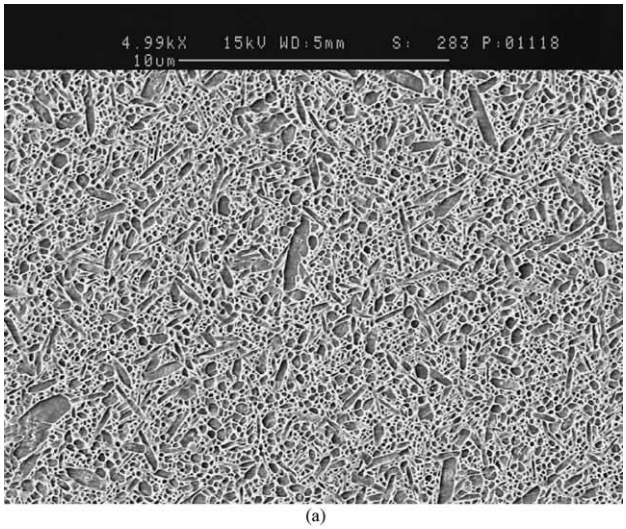

(a)

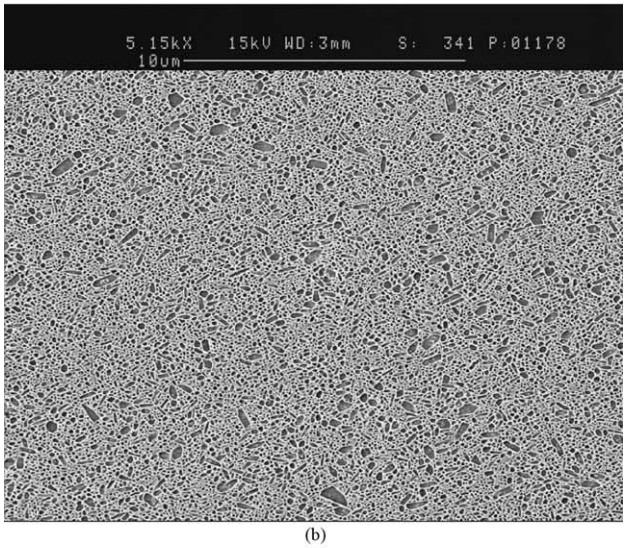

(b)

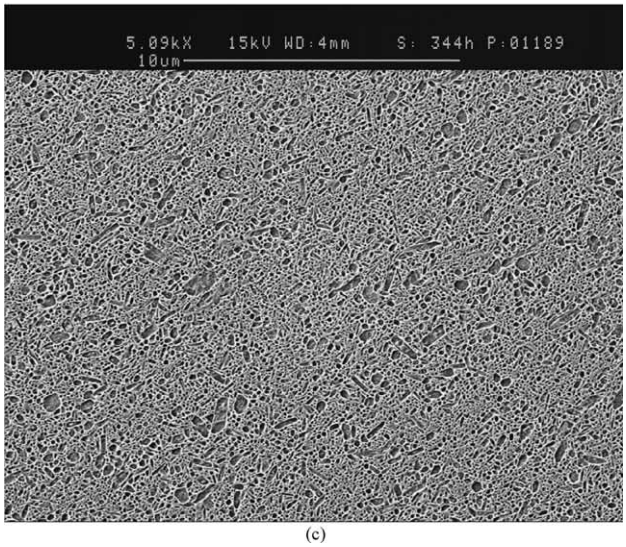

(c)

Fig. 5. SEM micrographs of etched, polished cross sections of hot-pressed materials (hot-pressing temperature: 1700 °C) of the powder SN-E10 (a), plasmachemical synthesised powder PP2 (b), and E10 and PP2 (50 wt.% SN-E10) (c).

materials derived from the fine β-Si_3N_4 powder were higher than that in the materials derived from the of the α powders. This is the reason, that at sintering temperatures of 1825 and 1900 °C the microstructures of the materials are similar, regardless of the α/β-ratio in the starting powder. To understand this behaviour the grain growth mechanisms of the β-Si_3N_4 grains has to be analysed.

In the literature it is well established that the different planes of the β-Si_3N_4 show different growth mechanisms—the basal {001} planes are atomically rough and the growth is diffusion-controlled whereas the {100} planes are atomically flat and interface-controlled growth was observed.[13–15] Due to the different growth mechanisms existing for different planes, the basal and prismatic planes show different dependencies of the growth rate on the oversaturation (Fig. 6). Anisotropic grain growth occurs at medium oversaturation, whereas isotropic grain growth occurs at very low degrees of oversaturation or at very high oversaturation. This is in agreement with the observed ratio of the growth rates in the length and thickness of 6–30 depending on the conditions.[13–16] The different faces of the crystal have also different stabilities. The basal planes {001} have higher surface energies than the prismatic planes {100};[13] i.e. the equilibrium concentration above the basal surfaces in the melt is higher than that above the prismatic planes (Fig. 7). Under the condition that the equilibrium surface concentration is lower than the overall concentration in the melt ($C < C_{melt}$), a crystal plane can growth. Therefore, large grains with high aspect ratios can grow in all directions, whereas small grains with lower aspect ratios dissolve. Crystals with intermediate size and aspect ratio can growth or dissolve in one or both directions.

The driving force for grain growth after the α to β transformation is indirectly proportional to the mean grain size.[17] In the case of very fine β-microstructures,

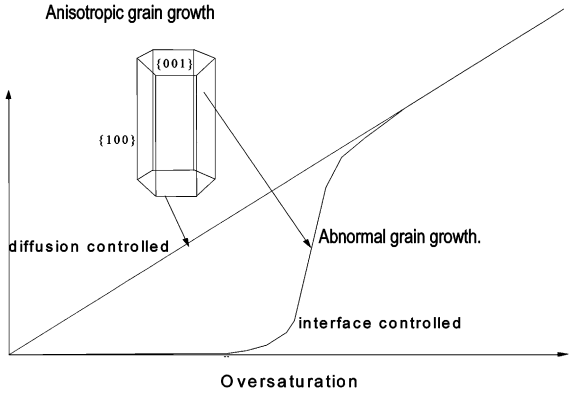

Fig. 6. Schematic view of the linear growth rate as a function of oversaturation for the basal planes {001} and the prismatic planes {100}.

the dependence of the oversaturation on the grain size is very strong. Therefore the largest grains grow also under high oversaturation, which is similar to what is observed during the α/β-transformation; whereas the grains in the microstructure with a large overall grain size growth under condition with only a low oversaturation. In Fig. 7a and b this is schematically shown for a coarse and a fine microstructure. This is the reason of the observed intensive anisotropic grain growth of the fine grained β-microstructures. However, with increasing grain size the oversaturation reduces and also the growth rate and the anisotropy of the growth rates reduces. This explains the observations in the 1970's and 1980's experimental results[18–20] that materials produced from powders with large β nuclei have more isotropic grain shapes than the materials based on α-powders: first, the anisotropic grain growth is less pronounced due to the very low oversaturation and secondly, the overall grain growth rate is much lower due to the coarser structure for this material, than for the high α-Si_3N_4 starting powders.[9]

On the basis of the results presented in the article and the data in the literature regarding microstructural design by seeding of materials with large needle-like β-grains,[21,22] the following schematic view can be proposed to show the influence of the amount and size of seeds on the microstructure formation (Table 5). Using fine β-particles as seeds, the microstructure can be controlled precisely. A wide range of microstructures can be developed by variation of sintering time and temperature.

Table 5
Dependence of the microstructure of the materials on the amount and size of the β-nucleus (T = temperature)

Powder			Microstructure	
β-Content	Crystallite size			
Wt.%	β	α	At the end of the α/β-conversion	Influence of sintering temperature and size
1–10	Fine < 100 nm	Fine ⩽100 nm	Needle like grains, aspect ratio decreases with increasing β-content and crystallite size, grain size decreases with decreasing crystallite size and increasing β-content	Low and medium T Fine grained with high aspect ratio High T Abnormal grain growth occur slow reduction of the mean Aspect ratio
> 30	Fine ⩽50–70 nm	Fine (⩽50–70 nm)	Very fine or nanosized microstructure with low aspect ratio, aspect ratio decreases with increasing β-content. Grain size decreases with decreasing crystallite size and increasing β-content	Low and medium T Increasing grain size and aspect ratio, slow change with increasing sintering time and T Medium and high T Grain size and aspect ratio increases; abnormal grain growth can occur
> 15–20	Coarse ⩾0.5–1 μm		Coarse grained microstructure with low aspect ratio	Low and medium T Coarse grained material with low aspect ratio; slow change with increasing sintering time and T High T Coarse grained material with low aspect ratio; slow change with increasing sintering time and T
1–10 + doping with 2–10% coarse β-seeds	Fine < 100 nm very coarse > 1–10 μm	Fine < 100 nm	Bimodal microstructure (large elongated grains in a fine grained matrix)	Low and medium T Slow or medium growth of the seeds with increasing sintering time and T High T Fast growth of the seeds (up to > 100 μm in length) with increasing sintering time and T formation of pronounced bimodal structure or material made only of large elongated crystals
1–10 + doping with < 30–50% fine β-seeds	Fine < 100 nm very fine < 20 nm	Fine < 100 nm	Microstructure very similar to a undoped microstructure	Microstructure very similar to a undoped microstructure

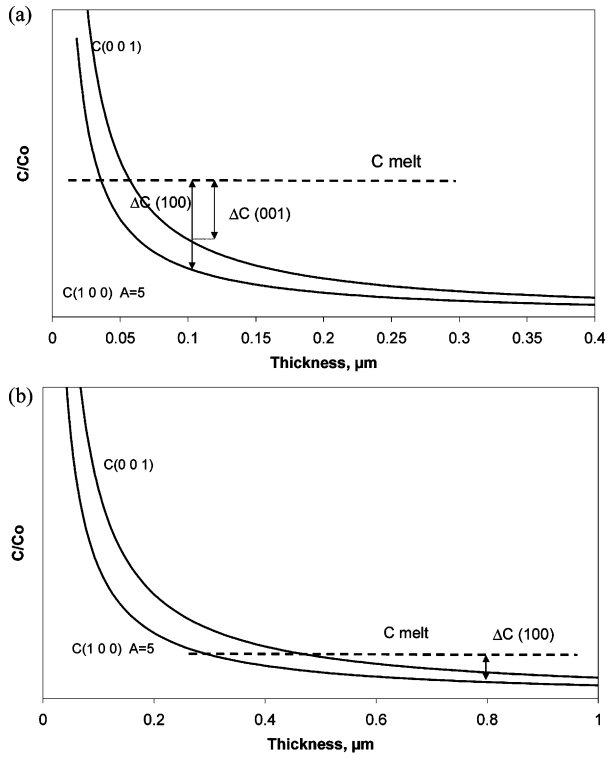

Fig. 7. Equilibrium concentrations above the basal (C(001)) and prismatic planes (C(100)) as a function of thickness of the β grains (the calculations are estimates based on the differences in surface energies calculated in Ref. 14; see Refs. 4,9 for further details). (a) Oversaturation ΔC above the {001} and {100} crystal planes of a crystal with a thickness of 0.1 μm in a material with an average grain size of about 50 nm and (b) of a grain with thickness of 0.8 μm in the melt 0.4 μm.

5. Conclusion

Fine-grained β-Si_3N_4 powders can be produced by crystallisation of plasmachemically produced powders in the presence of an oxynitride liquid. The covering of the nanosized particles by the oxynitride liquid improves the processing and reduces the oxygen pick up during the processing significantly.

The high sintering activity of the powders allows to separate the densification and adjustment of the microstructure. The resulting microstructures range from nanosized microstructures with equiaxed grains through microstructures with elongated grains to so-called in situ-reinforced microstructures. Fine-grained β-Si_3N_4 microstructures can also be produced by seeding α powders with fine-grained β-crystallites. This offers new possibilities for effective production of Si_3N_4 materials; e.g. after densification by gas-pressure sintering, superplastic deformation as a shaping process is possible. A subsequent heat treatment step can be performed to produce a microstructure consisting of elongated grains.

The formation of needle-like grains is a result of anisotropic grain growth occurring after α-to-β transformation. Therefore, after long sintering times and at high sintering temperatures, the microstructures of materials produced from β-powders are very similar to those produced from the α-powder.

The produced nanosized β-Si_3N_4 materials exhibit a high wear resistance and low friction coefficients which offers new possibilities for the use in ball bearings.

Acknowledgements

The authors are indebted to the co-workers in the IKTS especially to A. Bales, M. Ilgen K. Sempf, K. Nake involved in research projects or take part in the technical completion of the paper. The work for the microstructural design is based on a project supported by the DFG (wear resistant Si_3N_4 HE 2457/5-2) and on a running EU project concerning the quality control of plasmachemical synthesised Si_3N_4 and TiN powders.

References

1. Herrmann Petzow, M., Silicon nitride ceramics. In *Structure and Bonding*, Vol. 102. Springer Verlag; Berlin, Heidelberg, 2002, pp. 47–167.
2. Herrmann, M., Klemm, H. and Schubert, Chr., *Handbook of Ceramic Hard Materials*. Wiley-VCH 2, Weinheim, 2000.
3. Schulz, I., Herrmann, M., Reich, T. and Schubert, Chr., Siliciumnitrid—Werkstoffe mit niedrigem Reibungskoeffizient. *Tribologie und Schmierungstechnik*, 2003, **50**, 30–33.
4. Herrmann, M., Schulz, I., Schubert, Chr., Hermel, W., Zalite, I. and Ziegler, G., Ultrafine Si_3N_4 material with low coefficients of friction and wear rates, cfi/Ber. *DKG 75/4*, 1998, 38–45.
5. Suryanarayana, C., Structure and properties of nanocrystalline materials. *Bull. Mater. Sci.*, 1994, **17**(4), 307–346.
6. Chen, Z. *Engineering Ceramics 03*, Smolenice, 2003.
7. Niihara, K., New design Concepts of structural ceramics—ceramic nanocomposites. *J. Ceram. Soc. Jap.*, 1991, **99**, 974–982.
8. Herrmann, M., Schulz, I., Hermel, W., Schubert, Chr. and Wendt, A., Some new aspects of microstructural design of β-Si_3N_4 ceramics. *Z. Metallkd.*, 2001, **92**, 788–795.
9. Herrmann, M. and Schubert, Chr., Grundlagen der Gefügeausbildung in β-Siliciumnitrid werkstoffen. In *DKG Loseblattwerk Technische Keramische Werkstoffe, Kap. 5.1.3.1*, ed. J. Kriegesmann. Deutscher Wirtschaftsdienst, Köln, 1999.
10. Zalite, I. J. Europ. Ceram. Soc. (submitted for publication).
11. Anstis, G. R., Chantikul, P., Lawn, B. R. and Marshall, D. B., *J. Am. Ceram. Soc.*, 1981, **64**, 533–538.
12. Dressler, W., Kleebe, H.-J., Hoffmann, M. J., Rühle, M. and Petzow, G., *J. Europ. Ceram. Soc.*, 1996, **16**, 3–14.
13. Tien, T.-Y. and Hwang, C. J., *Mater. Sci. Forum*, 1989, **47**, 84–109.
14. M. Krämer, Untersuchungen zur Wachstumskinetik von β-Si_3N_4 in Keramiken und Oxinitirdgläsern. Dissertation, Stuttgart, 1992.
15. Tien, T.-Y., Ceramics. In *Silicon Nitride Ceramics, Mat. Res. Soc. Symp. 287. Mat. Res. Soc*, ed. I. W. Chen, P. F. Becher, M. Mitomo, G. Petzow and T. S. Yen, 1993, pp. 51–64.
16. Satet, R. Thesis. University Karlsruhe, 2003.
17. Wagner, C., *Zeitschrift für Elektrochemie*, 1961, **65**, 581–591.
18. Lange, F. F., *J. Am. Ceram. Soc.*, 1979, **62**, 428–429.

19. Wötting, G., Kanka, B. and Ziegler, G. *Nonoxide Ceramic*, 1986, 83–95.
20. Ziegler, G., Heinrich, J. and Wötting, G., *J. Mat. Sci.*, 1987, **22**, 3030–3041.
21. Hirao, K., Nagaoka, T., Brito, M. E. and Kanzaki, S., *J. Am. Ceram. Soc.*, 1994, **77**, 1857–1862.
22. Hirao, K., Nagaoka, T., Brito, M. E. and Kanzaki, S., *J. Ceram. Soc. Jpn.*, 1996, **104**, 55–59.